Carbohydrate Research 344 (2009) 85–90

Contents lists available at ScienceDirect

Carbohydrate Research

journal homepage: www.elsevier.com/locate/carres

The amorphous state of spray-dried maltodextrin: sub–sub-T_g enthalpy relaxation and impact of temperature and water annealing

Nicolas Descamps *, Stefan Palzer, Ulrich Zuercher

Nestlé Product Technology Centre, Lange Strasse 21, 78224 Singen, Germany

ARTICLE INFO

Article history:
Received 17 January 2008
Received in revised form 3 June 2008
Accepted 28 June 2008
Available online 6 August 2008

Keywords:
Glass transition
Physical ageing
Enthalpy relaxation
Spray-drying
Differential scanning calorimetry

ABSTRACT

The annealing behaviour of a spray-dried maltodextrin was investigated by differential scanning calorimetry. Special attention was paid to the effect of temperature and humidity on the annealing process. Comparison was also made with the glassy state of the same compound prepared by various cooling processes. The presence of a very pronounced sub-T_g peak upon ageing reveals the specificities of the glass and the complexity of the relaxation spectrum of the spray-dried material. This peak seems actually to correspond to a partial ergodicity recovery that may be attributed to onset of molecular mobility occurring below T_g. The position of the sub-T_g peak with regard to the conventional T_g was systematically studied. It clearly showed the difference between the effect of temperature and water plasticization on the relaxations occurring in the glassy state of materials prepared by spray-drying.

1. Introduction

Many solid compounds used in the pharmaceutical, chemical and food industries are produced and used in their amorphous glassy state. The classical way to produce a glass is to rapidly cool a melted compound. Below its melting temperature the liquid becomes metastable and falls out of equilibrium at the glass transition temperature (T_g). In industry, many formulation methods include other vitrification techniques. Vitrification may, for example, result from evaporation of solvent molecules as applied in freeze-drying[1] or spray-drying[2] processes. In all cases, the aim is to 'freeze' molecules in a liquid-like arrangement and to avoid crystallization. Direct solid state vitrification is also often observed upon milling[3] or micronisation.[4] During its formation, the glassy material is trapped in a local minimum of the potential energy landscape. The topology of this landscape characterizes the amorphous system. The physical state may strongly vary with the history of the material, that is, with the preparation process and the ageing. For example, in the classical quench cooling method to prepare a glass, the energy level where the end product is trapped depends on the cooling rate itself. Upon further ageing, the enthalpy of the system relaxes, and physical properties of the material are prone to change which may have a strong impact on characteristics such as reactivity,[5] solubility, hygroscopicity and mechanical material properties.[6]

The aim of this work is to demonstrate and clarify the specific thermodynamic properties of an amorphous compound obtained by spray-drying. Information on the amorphous state was obtained by investigating the effect of ageing conditions on the relaxation behaviour of the glass when heating it over the T_g. Glassy maltodextrin was chosen for this study as it is a good representative of an amorphous food or pharmaceutical material. It is also very sensitive to water uptake. Indeed, water plasticizes amorphous carbohydrates.[7] The importance of water plasticization in food has been initially recognized by Levine and Slade.[8,9] This property is used here to compare the effects of temperature and water content on the annealing behaviour of an amorphous carbohydrate matrix. A systematic investigation could be performed on the influence of the glass formation and ageing at different temperatures and relative humidities.

The differential scanning calorimetry (DSC) investigation of the spray-dried material points out the complexity of the relaxation spectrum in the sub-T_g temperature range. Systematic study of the effect of ageing on the configurational enthalpy and entropy allows to clarify the significance of the sub-T_g calorimetric events. The behaviour of spray-dried glasses is also compared with that of rapidly cooled glasses. The properties of the spray-dried glass and its eventual relaxations can be described in the frame of the energy landscape picture of the compound. Modulated differential scanning calorimetry (MDSC) provides additional information about slow molecular mobility associated with the sub-T_g calorimetric complexity. Comparison of the effect of the variation of temperature and relative humidity on the ageing relaxations has also been investigated. This led to compare the modifications induced by

* Corresponding author at present address: Department of Process and Chemical Engineering, University College, Cork, Ireland. Tel.: +33 684162067.
E-mail address: nicodescamps@hotmail.com (N. Descamps).

0008-6215/$ - see front matter © 2008 Elsevier Ltd. All rights reserved.
doi:10.1016/j.carres.2008.06.033

water on the relaxations which determine T_g and those which control ageing.

2. Materials and methods

Amorphous spray-dried (SD) maltodextrin DE21 (Glucidex® 21) (or solid dextrose syrup) was purchased from Roquette Frères (Lestrem, France) and stored for more than one year at 25 °C in air tight bags. Water activity a_w was 0.23 at 25 °C. Maltodextrin DE21 is a mixture of α-(1→4) linked glucose oligosaccharides with occasional α-(1→6) branches. Glucidex 21 is obtained by enzymatic hydrolysis of maize starch and its weight-average molecular weight M_w is 7260 Da. Its polydispersity index M_w/M_n is 7.41. The global impurity content is around 0.25%. Major impurities are proteins (⩽0.15%) and sulfated ashes (⩽0.1%).[10]

2.1. Experimental technique

The differential scanning calorimetry (DSC) experiments were performed using a Mettler-Toledo 822e calorimeter. The instrument was calibrated for temperature using the melting temperatures of indium (156.6 °C) and *n*-octane (−57 °C) and for heat flow using the heat of fusion of indium. The analyses were carried out on typically 10 mg of material hermetically sealed in preweighed aluminium pans of 40 μL. After each experiment, the tight seal of the pan was systematically checked by reweighing. Poor sealing induced water loss upon heating. The DSC oven was flushed with nitrogen gas. In order to analyze and compare the influence of various thermal treatments on the samples, all calorimetric measurements were performed at a standard heating rate of 5 °C/min. The reference T_g of each sample was defined as the midpoint of the glass transition heat flow jump of the corresponding normally cooled glass. The term 'normally cooled glass' refers here to a glass formed with a cooling rate of −5 °C/min.

Modulated DSC (MDSC Q1000 from TA Instruments) was also used in the 'heat only' mode (heating rate: 5 °C/min, oscillation period: 40 s, amplitude: 0.5 °C). This mode allows to investigate more accurately the influence of the thermal history of the sample separately on the reversing and the non-reversing components. In such an experiment, the maximum of the heat flow phase also enables to locate the temperature at which the time scale of the enthalpy relaxation equals that of the modulation.[11]

2.2. Experimental procedure

The spray-dried (SD) maltodextrin was annealed using different temperature and humidity conditions, which allows the amorphous state to evolve. A first DSC upscan was then performed up to temperatures above T_g (typically 30 °C above T_g) to analyze the effects of such treatments through changes in the heat flow behaviour in the vicinity of T_g. Above T_g, the amorphous state is expected to recover its internal metastable equilibrium. To compare with the state of a normally cooled glass, the sample was then cooled down slowly to 45 °C below T_g (−5 °C/min) and heated up again in a second upscan at 5 °C/min. Such a thermal treatment allowed the determination of the value of configurational enthalpy and entropy of the two types of glasses: the annealed one and the normally cooled one. Similar comparison was also made for spray-dried (SD) glass and rapidly cooled (RC) glass. Rapid cooling was achieved by placing directly the hot sealed pan containing sample (130 °C) in air at room temperature.

For temperature annealing, samples were heated directly in the DSC pan. For humidity annealing, samples were equilibrated for 6 months at 23 °C and at various relative humidities (RH) in desiccators containing saturated salt solutions of known RH values (RH = 11% (LiCl), 23% (CH_3COOK), 33% ($MgCl_2$), 43% (K_2CO_3) and 53% ($Mg(NO_3)_2$)). Solutions were prepared by dissolving salts provided by Fluka Chemie AG in demineralized water. Humidity equilibration of the samples was checked measuring their water activity. Water activity was measured in duplicate using a humidity sensor (HygroPalm AW1 from Rotronic) at 25 °C, which was calibrated with standard salt solutions provided by Rotronic AG/CH.

3. Results and discussion

3.1. Spray-dried maltodextrin: calorimetric behaviour

Figure 1A shows the first and second upscans (respectively, curves (a) and (b)) of a maltodextrin sample prepared by spray-drying and stored at 23 °C, 23% RH for more than one year. The second upscan (normally cooled glass without ageing) reveals a clean C_p jump indicating a glass transition situated at T_g = 86 °C. On the contrary, the first upscan exhibits an endothermic peak at T'_m = 73 °C. This peak is followed by a C_p jump which looks similar to that of a conventional glass transition (as observed on curve (b)), but shifted towards higher temperature—compared to the normally cooled glass. The two curves superimpose well above and well below T_g. First and second upscans of modulated DSC (MDSC) experiments are presented in Figure 2. Reversing heat flow signals for both SD and normally cooled glasses show heat flow jumps classically expected at glass transition. There is no evident temperature shift of the reversing signal for both SD and normally cooled glasses. In other words, the glass transition temperature is the same for SD and normally cooled glasses. This means that the onset of mobility essentially occurs at the same temperature in both cases. This behaviour contrasts with the apparent T_g shift of the average heat flow (HF) signals seen in Figure 1. Consequently, the non-reversing HF signal for the SD glass shows a well-

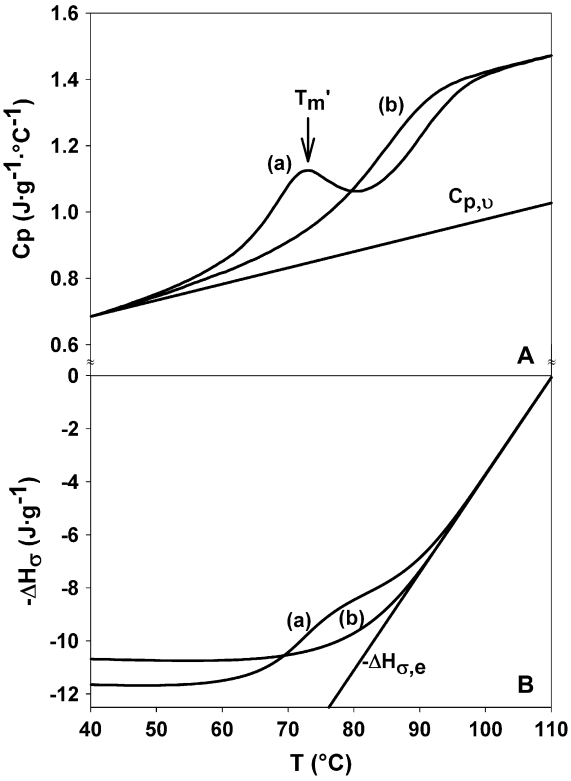

Figure 1. The heat capacity, C_p [A], and the corresponding configurational enthalpy $-\Delta H_\sigma$ [B] of maltodextrin DE21 after various heat treatments. The scanning rate is 5 °C/min. (a) SD maltodextrin. (b) Normally cooled glass after slow cooling from 120 °C (−5 °C/min).

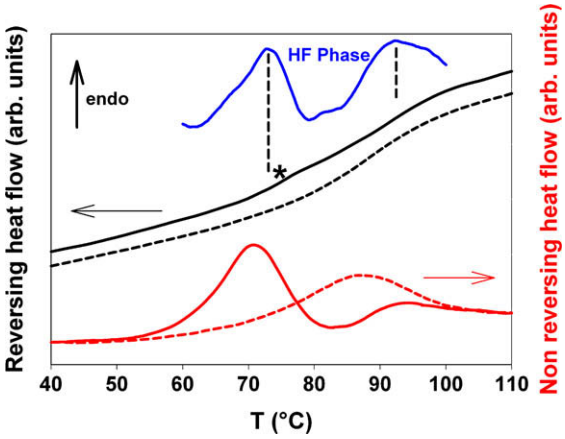

Figure 2. Reversing and non-reversing heat flow curves obtained by MDSC for the spray-dried maltodextrin (first upscan—full curves) and normally cooled glass (second upscan—dashed lines). The star signals the slight break in the reversing heat flow corresponding to the sub-T_g peak. Reversing signals were shifted vertically for clarity. Heat flow phase peaks for the first upscan are also reported.

pronounced endothermic sub-T_g peak, which is followed by a clear exothermic contribution event. It is to be noticed that the non-reversing signal of the normally cooled glass displays a peak at about 87 °C, whereas its average HF does not show any overshoot. However, such a peak does not indicate any pronounced structural relaxation event. As noticed by Bustin et al.,[11] it is mainly a consequence of the way the non-reversing contribution is built. Indeed, the latter is simply the difference between the average heat flow and the reversing component. Both have glass transition temperatures which differ slightly because their corresponding sweeping rates are different. This T_g difference gives rise to a non-significant maximum in the non-reversing component. A closer look at the reversing HF signal of the first upscan shows a slight, but reproducible change in the slope in the temperature zone of the endothermic event.

Sub-T_g heat capacity peaks were reported for a large variety of rapidly cooled glasses which have been pre-annealed at very low temperature such as polymers,[12–15] metals,[16,17] oxides[18] and silicates.[19,20] Occurrence of such features has also been recently discussed by Johari,[21,22] Yue and Angell[23] related to T_g of water. Glasses showing these features have been obtained by a variety of rapid cooling techniques such as those which are used in the production of glass fibres,[19,20,23] but also vapour deposition.[17] In the case of polymers, it has also been mentioned that the freeze-drying process may produce glasses showing such a sub-T_g endotherm.[1] We show here that spray-drying is a vitrification technique that produces glasses having a sub-T_g peak and thus having the thermodynamic signature of rapidly cooled glasses. Similar observations have been made for other rapidly quench-cooled amorphous food products (polysaccharides,[24] sugars[25] and starch[26]) which indicates that such behaviour is rather general for industrially prepared glasses.

3.2. Comparison of calorimetric behaviour of spray-dried/rapidly cooled materials

To investigate further the effective conditions of vitrification by spray-drying, DSC experiments were performed on glassy maltodextrin which were obtained by slow (−5 °C/min) and rapid cooling from temperature above T_g. Rapid cooling was achieved by cooling the sample in a sealed pan directly from 130 °C to room temperature. The corresponding cooling rate was estimated to be −380 °C/min based on a systematic study of the evolution of the fictive temperature as a function of the cooling rate as proposed

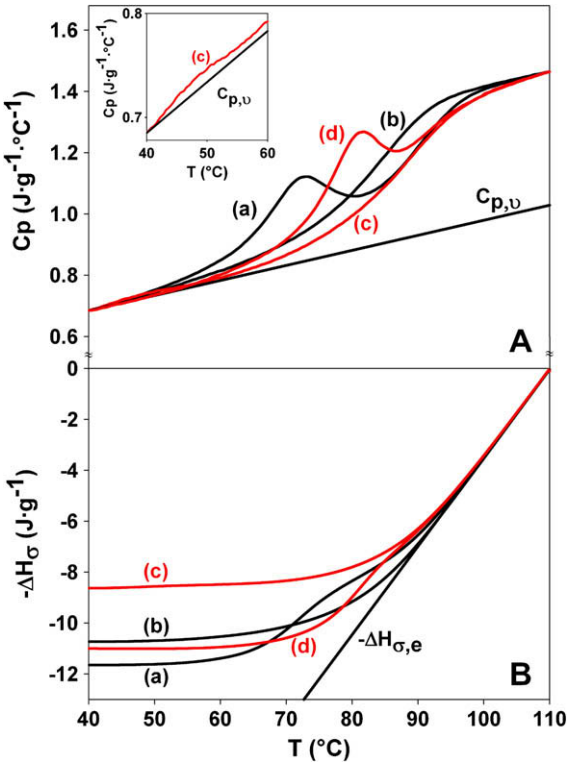

Figure 3. The heat capacity, C_p [A], and the corresponding configurational enthalpy $-\Delta H_\sigma$ [B] of maltodextrin DE21 after various heat treatments. The scanning rate is 5 °C/min. (a) SD maltodextrin. (b) Normally cooled glass. (c) RC glass (−380 °C/min) after a short ageing period (≈30 min) at T_a = 25 °C. The inset shows a close-up view of the sub-T_g peak region. (d) RC glass (−380 °C/min) after being annealed 20 h at T_a = 55 °C.

by Velikov et al.[27] Incidentally, such investigation allows an estimation of the fragility index (m) of the compound. We found m = 117. The fragility index has been defined as a distinctive property that characterizes dynamic relaxations at molecular level in glass forming liquids. In practice, it is quantified by the dependence of relaxation times on temperature changes in the region approaching the glass transition. With an m value higher than 100, maltodextrin DE21 fits within the class of a fragile liquid following the strong/fragile classification.[28]

Figure 3A shows upscans at 5 °C/min performed on RC glasses, after a short (≈30 min) annealing period at room temperature (curve (c)) and 20 h annealing at 55 °C (curve (d)). Upscans of SD (a) and normally cooled (b) materials are also reported for comparison. On curve (c) a slight, but clear sub-T_g endotherm can be observed between 40 °C and 50 °C (see a close-up view in inset). At higher temperature, a temperature shift of the C_p curve of about 4 °C with regard to that of the normally cooled glass (curve (b)) can be noticed. Such a shift is similar to that observed on the SD material (curve (a)). On curve (d) a well pronounced sub-T_g peak is observed at 82 °C (9 °C above that of the SD material). At higher temperature, a superimposition with the C_p curve of the SD product is also observed. All these features indicate that the effective cooling rate produced during spray-drying is similar to that of the RC cooled sample. These results further demonstrate that RC as well as SD samples is able to produce sub-T_g endothermic peaks at very low temperatures and that the position of these peaks is very sensitive to ageing.

3.3. Analysis of the energy landscape of SD and RC dextrose

At a temperature low enough below T_g, the contributions to C_p are mainly those of the fast vibrational degrees of freedom, as slow

and large amplitude-configurational motions are frozen.[29] Since all C_p curves superimpose well below T_g, the events revealed in the range 100 °C > T > 40 °C can be attributed to configurational contributions which are dependent on thermal history. Configurational contributions to C_p are in addition to the low-temperature vibrational specific heat capacity $C_{p,v}$.[12] The values of $C_{p,v}(T)$ are obtained by extrapolation from values of C_p below 40 °C as shown in Figures 1A and 3A.

To examine the significance of the sub-T_g effect, the configurational enthalpies

$$\Delta H_\sigma(T) = -\int_{110}^{T}(C_p - C_{p,v})\mathrm{d}T \quad (1)$$

are shown in Figures 1B and 3B. Here, $\Delta H_{\sigma,e}(T)$ is the ΔH_σ of the undercooled equilibrated liquid, and is set to be zero at 110 °C. At low temperature $-\Delta H_\sigma$ of the RC sample decreases upon ageing. Upon heating, the $-\Delta H_\sigma$ of the annealed RC sample increases towards the non-aged RC value (curve (c)) and merges with it below T_g. Upon heating, the system thus recovers the enthalpy level trapped at T_g upon cooling, before undergoing the glass transition. Same behaviour is seen for the annealed SD glass (curve (a)). The low temperature configurational enthalpy value is slightly lower than that of the aged RC sample. Upon heating, it increases towards curve (c) and nearly merges with it well below T_g. This shows that the enthalpy levels trapped upon rapid cooling or during fast dehydration are most probably of similar values even if the preparation processes are different. Note that the configurational enthalpy curves always stay on the left of the equilibrium line $-\Delta H_{\sigma,e}$ before merging with it. This behaviour differs from what is usually observed for sub-T_g annealing, which results in a peak of C_p and fast recovery of enthalpy just above T_g ('ageing overshoot').[30]

The low enthalpy levels of the glassy samples with different histories (glass formation and annealing) are directly read on the left-hand side of the picture. They reflect the corresponding values of the fictive temperature of the glass. The latter are given by the temperature of intersection of the equilibrium line $-\Delta H_{\sigma,e}(T)$ with the line corresponding to the enthalpy of the glass. The enthalpy of the glass is extrapolated from values of $\Delta H_\sigma(T)$ below T_g.[31] After long annealing at a temperature below T_g, the fictive temperature of the SD material is lower than that of the RC glass. It has even a lower value than that of the normally cooled glass. However, this does not produce—as usually expected after a sub-T_g annealing—a fast recovery on the right-hand side of the equilibrium line and the corresponding C_p overshoot.[30] On the contrary, the glass tries to catch up with a faster cooling rate curve before crossing the equilibrium line. Incidentally this feature indicates that the fictive temperature value is not capable by itself to determine the ultimate behaviour of a glass upon heating. This supports the fact that the structural state of the SD glass has specific features associated with its manufacturing process.

Amorphous systems can be described in terms of a potential energy landscape with a multitude of minima, which are separated by energy barriers of various heights.[32,33] Each of these minima controls the thermodynamics and corresponds to a particular glass structure. The structural transition rate is determined by the barrier height. When a glass is formed, it is trapped in a region of the landscape which depends on the vitrification route and has a specific local topology. The possible behaviours that are observed upon both ageing and reheating correspond to different paths in the complex energy landscape which start at a specific trap location. Upon ageing the glass relaxes to lower reachable energy states. The fictive temperature (T_f) displays an energy level of the glass which equals that of the equilibrium liquid at this temperature. Properties other than those reflected in the value of T_f certainly influence the behaviour of glass upon heating. They concern the energy barriers that are felt by the system at some point of the trajectory on the landscape as well as its roughness (number of minima).

It is thus interesting to consider the evolution of entropy (S) which reflects the number of accessible configurational states. The change in the slope of the configurational enthalpy curves implies similar changes in the slope of the configurational entropy curves $\Delta S_\sigma(T)$ as a function of temperature. This is reflected by

$$\frac{\partial \Delta H}{\partial T} = T\frac{\partial \Delta S}{\partial T} \quad (2)$$

Integration of Eq. (2) leads to the configurational entropy curves shown in Figure 4.

The recovery of H observed on the left-hand side of the equilibrium $-\Delta H_{\sigma,e}$ line is thus accompanied by an increase of S also occurring on the left-side of the equilibrium line $-\Delta S_{\sigma,e}$. Such an entropy jump is the result of a rapid increase in phase space by which new molecular configurations become accessible. The sub-T_g peak accompanies the possibility that the system has to explore a larger zone of the phase space. The value of H measured above the sub-T_g peak thus corresponds to a statistical averaging on this accessible part of the phase space. In other words, the sub-T_g peak is the signature of a partial recovery of ergodicity.

The enthalpy recovery, which clearly occurs below T_g, needs the onset of molecular mobility activated at this temperature. The reversing heat flow signal exhibits a slight break (cf. star in Fig. 2) that can be attributed to such an onset of molecular mobility occurring below T_g. This is confirmed by the evolution of the heat flow phase (cf. Fig. 2) which shows two peaks revealing two enthalpy relaxation processes occurring on the time scale of the modulation: the first one occurs in the temperature range of the sub-T_g peak and the other one in the range of the glass transition of the normally cooled glass. Sub-T_g mobility can potentially be attributed either to secondary β-relaxations or to some specific contribution from the distributed main α-relaxations. On the time window of calorimetric investigations, β-relaxations are expected to be activated at temperatures much lower than T_g. They are typically situated in the temperature range where thermo-stimulated depolarization currents (TSDC) experiments display them.[34] Furthermore, Figure 5 shows a continuous evolution of the sub-T_g peak location as a function of annealing until reaching T_g. The detected onset of sub-T_g mobility is thus more likely to be associated to a low energy-activated component of the α-relaxations spectrum. Such a contribution would be enhanced by the SD vitrification pro-

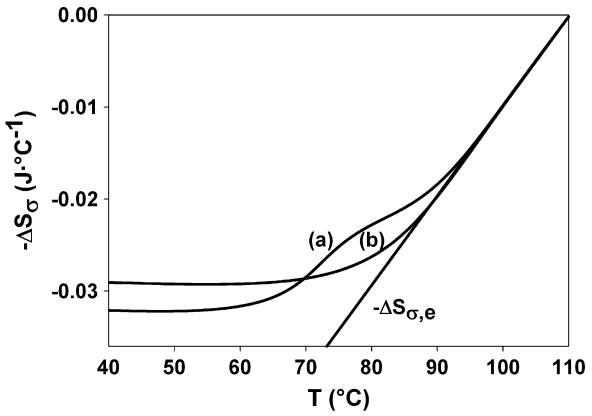

Figure 4. Configurational entropy $-\Delta S_\sigma$ of maltodextrin DE21 after various heat treatments. The scanning rate is 5 °C/min. (a) SD maltodextrin. (b) Normally cooled glass.

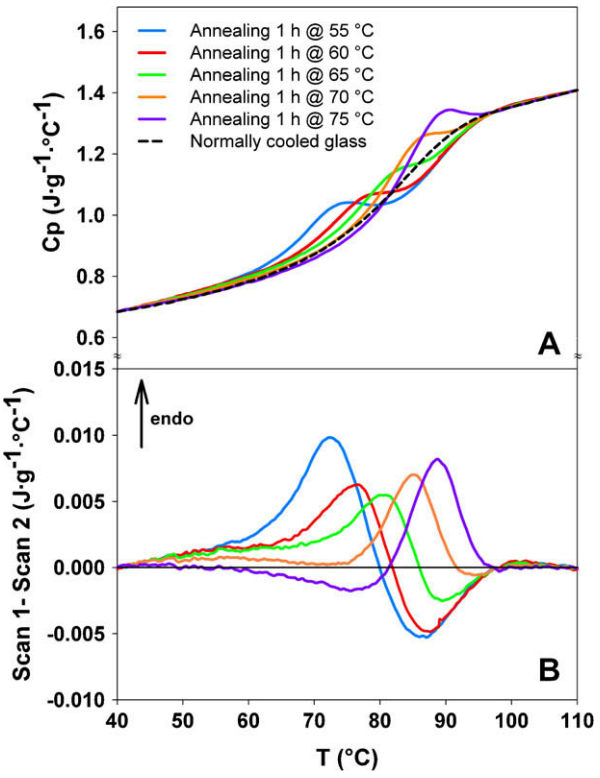

Figure 5. The heat capacity, C_p [A], and the difference between the first and second upscans [B] of the spray-dried maltodextrin after annealing time of 1 h at different temperatures (55 °C < T_a < 75 °C). The sub-T_g peak temperature increases with the annealing temperature.

cess, which traps the system in energy landscape regions where relaxation barriers are relatively low.

3.4. Influence of ageing temperature (T_a) and relative humidity (RH) on the annealing behaviour

Temperature and water content have a great impact on the behaviour of amorphous carbohydrates during storage. Therefore, systematic calorimetric experiments were performed on spray-dried maltodextrin aged at different temperatures and humidities. The aim of the study was to see the impact of the temperature and water plasticization on the relaxation of glasses. The results of this study are presented in Figures 5 and 6.

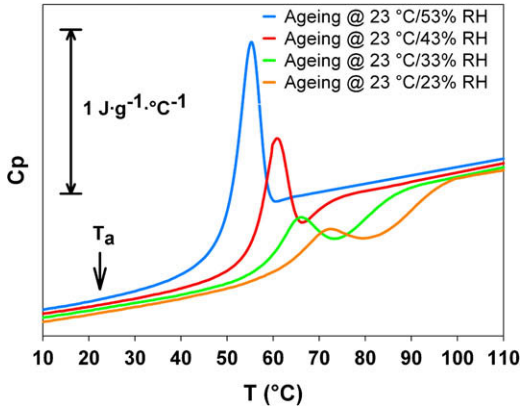

Figure 6. The heat capacity, C_p, of the spray-dried maltodextrin after annealing time of 6 months at 23 °C and different RHs. These curves evidence both plasticization effect of water (decrease of T_g with increasing RH) and the evolution of the position of the sub-T_g peak relatively to T_g. Heat flow signals were shifted vertically by a constant offset for clarity.

3.4.1. Influence of the ageing temperature

Figure 5 illustrates the effect of annealing temperature T_a (varying from 55 °C to 75 °C) on the structural relaxation behaviour of spray-dried maltodextrin equilibrated at 23% RH for a given annealing time (t_a) of 1 h. To better visualize the development of the endothermic and exothermic events, the second upscan has been subtracted from the first upscan (Fig. 5B).

As observed in Figure 1A, the first upscans of the annealed samples shown in Figure 5A present an endothermic sub-T_g peak, whereas a classical C_p jump appears on the second upscan. Increasing the annealing temperature (T_a) induces a progressive shift of the sub-T_g peak temperature T'_m to higher temperatures. It is to be noted in Figure 5B that this shift of T'_m corresponds to a gradual decrease of the width of the exotherm until it totally disappears. Another observation concerns the regular increase of T'_m when T_a increases. Figure 7 demonstrates that this increase is linear. Such a linear evolution has also been reported by Hodge.[13] Interpreted in terms of energy landscape, this behaviour is explained by the fact that lower energy levels are reached with a concomitant increase of barrier heights. That leads to recovery relaxations which are activated at higher temperatures. Hodge[13] also mentioned that the peak height evolves linearly with T_a. Such a linear evolution of the peak height may only be seen here when the annealing temperature exceeds 65 °C. Indeed, the peak height first decreases when T_a increases and then linearly increases. This effect may be due to the fact that enthalpy recovery starts between 55 °C and 60 °C. The system recovers the high energy level on the left of the equilibrium line $-\Delta H_{\sigma,e}$ without any ageing compensation (Fig. 1B). Indeed, the annealing process is too slow at the lowest temperatures (55 °C, 60 °C and 65 °C) to compensate the enthalpy recovery within one hour. On the other hand, at higher temperatures (70 °C and 75 °C), relaxation times become shorter which enables compensation of the energy recovery by enthalpy relaxation.

3.4.2. Influence of the relative humidity on ageing

Water has a great influence on the position of the glass transition temperature of maltodextrin.[7] The annealing of maltodextrin

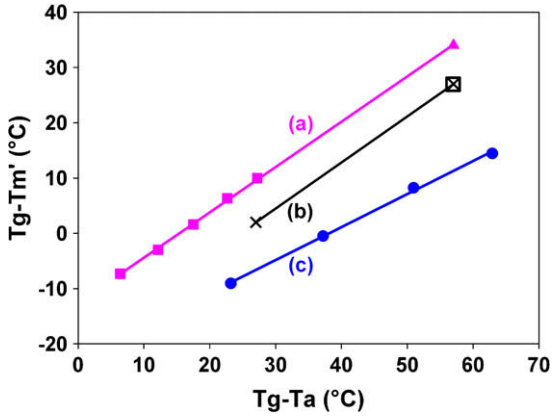

Figure 7. Evolution of the difference between the glass transition temperature, T_g, and the peaking temperature of the endotherm, T'_m, as a function of the difference between T_g and the annealing temperature, T_a. (a) ■ SD maltodextrin annealed for 1 h at different temperatures: T_a = 55 °C, 60 °C, 65 °C, 70 °C and 75 °C. ▲ RC material annealed for 1 h at T_a = 25 °C. Direction coefficient of the regression line = 0.82. (b) RC material annealed for 20 h at different temperatures: ⊠ T_a = 25 °C and × T_a = 55 °C. Direction coefficient of the regression line = 0.83. (c) ● SD maltodextrin annealed for 6 months at 23 °C and different relative humidities: RH = 23%, 33%, 43% and 53%. Direction coefficient of the regression line = 0.59.

at different RH conditions was investigated. This allows changing the relative position of the annealing temperature with regard to T_g. Figure 6 presents the thermograms obtained after a long annealing period of 6 months at 23 °C and different humidity conditions (23% < RH < 53%).

The tendency observed here in the evolution of the sub-T_g peak temperature is the same as the one observed above while changing the annealing temperatures (see Fig. 5). Indeed, such as temperature, water plasticizes the matrix. Thus, the glass transition temperature T_g of the initial material decreases and the difference between T_g and T_a decreases as well. This causes a decrease of the difference $T_g - T'_m$ (from $T_g - T'_m = 14$ °C at 23% RH to $T_g - T'_m = -9$ °C at 53% RH, see Fig. 7). This difference becomes even negative for the lowest T_g value as it is observed in the usual sub-T_g annealing.[30] Plotting the evolution of $T_g - T'_m$ as a function of $T_g - T_a$, a linear evolution is obtained similar to the one observed for temperature ageing (see Fig. 7).

3.5. Comparison between temperature and water plasticization effects

Figure 7 compares the influence of two ageing conditions on the relaxation process of maltodextrin: temperature ageing (lines (a) and (b)) and water ageing (line (c)). It first appears that, regardless of the annealing process, $T_g - T'_m$ evolves linearly with $T_g - T_a$. However, the slopes and the positions of the lines are quite different. Lines (a) and (b) show the effect of increasing the annealing time from 1 h to 20 h. Their parallel shift corroborates the findings of Hodge[13] that the peaking temperature increases approximately linearly with $\log(t_a)$. During annealing at different humidities, the annealing time was 6 months which leads to even smaller $T_g - T'_m$ values. It is to be noted on line (a) that the point corresponding to an annealing temperature $T_a = 25$ °C (i.e., $T_g - T_a = 57$ °C, right-hand side of the line) results from the ageing of an RC sample. The alignment of this point with those obtained after annealing SD samples as well as the parallelism of lines (a) and (b) further demonstrates the similarity of the sub-T_g relaxations of the two samples SD and RC.

The difference in slope of line (c) demonstrates that annealing at a temperature closer to T_g by increasing the temperature or the relative humidity is not equivalent in terms of molecular relaxation. Indeed, T'_m increases more significantly relative to T_g using temperature plasticization compared to water plasticization. This result could mean that temperature increase makes the glass sink more rapidly in the energy landscape than the increase in water content does. In other words, upon ageing, temperature plasticization is more efficient to release energy than water plasticization.

This difference may be correlated to what was already observed by Zheng et al.[14] who concluded that: 'the hypothesis 'the change of relative humidity has similar effects to temperature changes on the physical ageing response of glassy polymers' is qualitatively correct. Quantitatively, however, the kinetics of structural recovery in RH-jump and T-jump histories are anomalously different in that the RH-jump experiment results in longer structural recovery times'. Zheng et al.[15] also stated that when comparing the viscoelastic responses between RH-jump and T-jump to the same final conditions, the responses after the T-jump have a smaller characteristic retardation time and a larger physical ageing rate than after the RH-jump. In the present case, the qualitative equivalence between the effect of temperature and relative humidity is reflected by the difference of position between lines (a) and (c). The quantitative difference between the kinetics of recovery in RH jump and T jump histories is clearly reflected by the difference of slope between lines (a), (b) and (c).

4. Conclusion

The specific heat data on annealed spray-dried maltodextrin show a sub-T_g endotherm, suggesting a glass structure equivalent to the one observed for rapidly cooled materials. Furthermore, this sub-T_g peak seems to correspond to a partial ergodicity recovery that may be attributed to some onset of molecular mobility occurring below T_g. Enthalpy interpretation of the presence of maxima and minima in specific heat at temperatures below T_g reveals the complexity of the relaxation spectrum of spray-dried glassy maltodextrin. Moreover, it was shown that a fictive temperature value is not capable by itself to determine the ultimate behaviour of the present glassy system upon heating. In addition, study of the evolution of the enthalpy relaxation upon ageing at different temperatures and relative humidities shows that temperature plasticization is more efficient than water plasticization to enhance relaxations below T_g. This means that at the same temperature gap between T_a and T_g, the kinetics of structural recovery is better enhanced by an increase of temperature than by an increase of water content.

Acknowledgements

The authors are grateful for the support of the European Union Commission through the 'BioPowders' Marie Curie Research Training Network. Professor Y. H. Roos, P. Vadi and S. Krause are thanked for a critical reading of the manuscript. Thanks are also due to Roquette Frères for the detailed information provided on Glucidex® 21.

References

1. Shultz, A. R.; Young, A. L. *Macromolecules* **1980**, *13*, 663–668.
2. Roos, Y. H. *Lait* **2002**, *82*, 475–484.
3. Willart, J. F.; Descamps, N.; Caron, V.; Capet, F.; Danède, F.; Descamps, M. *Solid State Commun.* **2006**, *138*, 194–199.
4. Cook, P. A.; Dellman, C. I.; Horspool, K. R.; Lukas, T. M.; Marshall, P. V.; Nichols, G.; Smith, D.; Ticehurst, M. D. *Eur. J. Pharm. Sci.* **1996**, *4*, 181.
5. Liu, J.; Rigsbee, D. R.; Stotz, C.; Pikal, M. J. *J. Pharm. Sci.* **2002**, *91*, 1853–1862.
6. Noel, T. R.; Parker, R.; Brownsey, G. J.; Farhat, I. A.; MacNaughtan, W.; Ring, S. G. *J. Agric. Food Chem.* **2005**, *53*, 8580–8585.
7. Kilburn, D.; Claude, J.; Schweizer, T.; Mezzenga, R.; Dlubeck, G.; Alam, A.; Ubbink, J. *J. Phys. Chem. B* **2004**, *108*, 12436–12441.
8. Levine, H.; Slade, L. In *Water Science Reviews*; Franks, F., Ed.; Cambridge University Press: Cambridge, 1988; Vol. 3, pp 79–185.
9. Slade, L.; Levine, H. *Pure Appl. Chem.* **1988**, *60*, 1841–1864.
10. Roquette Frères, Glucidex® 21 Data Sheet 2008.
11. Bustin, O.; Descamps, M. *J. Chem. Phys.* **1999**, *110*, 10982–10992.
12. Chen, H. S.; Wang, T. T. *J. Appl. Phys.* **1981**, *52*, 5898–5902.
13. Hodge, I. M. *J. Non-Cryst. Solids* **1994**, *169*, 211–266.
14. Zheng, Y.; McKenna, G. B. *Macromolecules* **2003**, *36*, 2387–2396.
15. Zheng, Y.; Priestley, R. D.; McKenna, G. B. *J. Polym. Sci. Part B: Polym. Phys.* **2004**, *42*, 2107–2121.
16. Chen, H. S.; Inoue, A. *J. Non-Cryst. Solids* **1984**, *61–62*, 805–810.
17. Stephens, R. B. *J. Appl. Phys.* **1978**, *49*, 5855–5864.
18. Chen, H. S.; Kurkjian, C. R. *J. Am. Ceram. Soc.* **1983**, *66*, 613–619.
19. Yue, Y. Z.; Jensen, S. L.; Christiansen, J. d. *Appl. Phys. Lett.* **2002**, *81*, 2983–2985.
20. Yue, Y. Z. *Phys. Chem. Glasses* **2005**, *46*, 354–358.
21. Johari, G. P. *J. Phys. Chem. B* **2003**, *107*, 9063–9070.
22. Johari, G. P. *J. Chem. Phys.* **2003**, *119*, 2935–2937.
23. Yue, Y.; Angell, C. A. *Nature* **2004**, *427*, 717–720.
24. Borde, B.; Bizot, H.; Vigier, G.; Buleon, A. *Carbohydr. Polym.* **2002**, *48*, 111–123.
25. Borde, B.; Cesàro, A. *J. Therm. Anal. Calorim.* **2001**, *66*, 179–195.
26. Thiewes, H. J.; Steeneken, P. A. M. *Carbohydr. Polym.* **1997**, *32*, 123–130.
27. Velikov, V.; Borick, S.; Angell, C. A. *J. Phys. Chem. B* **2002**, *106*, 1069–1080.
28. Angell, C. A. *J. Non-Cryst. Solids* **1991**, *13*, 131–133.
29. Slade, L.; Levine, H. *Crit. Rev. Food Sci. Nutr.* **1991**, *30*, 115–360.
30. Liu, Y.; Bhandari, B.; Zhou, W. *J. Agric. Food Chem.* **2006**, *54*, 5701–5717.
31. Moynihan, C. T.; Easteal, A. J.; DeBolt, M. A.; Tucker, J. *J. Am. Ceram. Soc.* **1976**, *59*, 12.
32. Debenedetti, P. G.; Stillinger, F. H. *Nature* **2001**, *410*, 259–267.
33. Sastry, S.; Debenedetti, P. G.; Stillinger, F. H. *Nature* **1998**, *393*, 554–557.
34. Correia, N. T.; Alvarez, C.; Moura Ramos, J. J.; Descamps, M. *Chem. Phys.* **2000**, *252*, 151–163.